ORIGINAL PAPER

Chinmoy Bhattacharya · Jayati Datta

Synthesis of nanostructured Cd–Se–Te films through periodic voltammetry for photoelectrochemical applications

Abstract In the present investigation, polycrystalline semiconductor Cd–Se–Te films have been electrodeposited at room temperature on conducting glass substrates using cyclic voltammetric technique under controlled periodic scans. The successive anodic and cathodic scans were recorded within the potential range, from 0 to −1.0 V, and over the range of periodic cycles, from 250 to 2,000, in an acidic bath containing respective reducible precursor ions like Cd^{2+}, Se^{4+}, Te^{4+}, and 1 vol.% Triton X-100 as the surface-active reagent. Thin composite films were produced having variable thickness and composition and grain size of the order of 80–100 nm. The film properties were determined by focused ion beam analysis, energy dispersive analysis of x-rays, x-ray diffraction studies, atomic force microscopy, and scanning electron microscopy. Thickness of the semiconductor films was found to increase linearly with the number of voltammetric cycles. Band gap energies of the films as derived from the reflectance spectra were found to lie between 1.4 and 1.7 eV. The composite films of the Cd–Se–Te ternary system when electrochemically characterized in aqueous polysulfide solution exhibited n-type semiconducting properties and photoconversion efficiency more than 0.4%.

Keywords Cd chalcogenides · Thin films · Electrochemical techniques · Interfacial electrochemistry · Surface morphology

Introduction

Polycrystalline II–VI binary semiconductor (SC) compounds belonging to the cadmium chalcogenide family (CdS, CdSe, and CdTe) are considered to be technologically important materials for applications in optoelectronic devices and solar cells, because they possess specific physical properties such as direct bandwidth, high absorption coefficient in the visible and infrared part of the solar spectrum, good electrical properties, and increased capability in obtaining adjustable n- or p-type conductivity by suitable doping elements [1–5]. Particularly, the selenides and tellurides of Cd possessing band gap energies of 1.7 and 1.4 eV, respectively, are advocated as potential candidates for the conversion of low energy light into electricity. Furthermore, intercombinations of these SC compounds often produce interesting ternary systems with controlled bandwidths depending on their compositions [2, 6–9].

A great deal of attention has been focused on the fabrication of SC thin films with chalcogenide materials by various routes like chemical deposition, vacuum evaporation, and cathodic deposition [2, 6–19]. The present work involves synthesis of polycrystalline SC films comprising mixed/alloyed Cd–Se–Te compounds on conducting glass substrates by employing an electrochemical technique, which has rarely been used so far and is based on cyclic voltammetry under controlled number of scans. In the course of successive evaluation of optical, microstructural, and photoelectrochemical (PEC) properties of the various codeposited films having different compositions of Cd, Se, and Te in the matrix, the most suitable one was identified for liquid-junction solar cell applications.

Materials and methods

Synthesis of the semiconductor films on conducting glass substrates

Thin films of the SC system Cd–Se–Te were electro-synthesized through periodic voltammetry on transparent conducting oxide (TCO, fluorine-doped SnO_2) coated glass substrate supplied by BHEL, India. The electrochemical bath contained analytical grade reagents like $CdCl_2$ (0.2 M), SeO_2 (1×10^{-3} M), and TeO_2 (1×10^{-3} M) as the

C. Bhattacharya · J. Datta (✉)
Department of Chemistry,
Bengal Engineering & Science University,
Shibpur, 711103 Howrah,
West Bengal, India
e-mail: jayati_datta@rediffmail.com
Tel.: +91-033-26684561
Fax: +91-033-26682916

precursor compounds in aqueous solution. TeO_2 was first dissolved in concentrated H_2SO_4 and then diluted with water to maintain the pH of the working solution at 2, and Triton X-100 (1 vol.%) was used as surface-active reagent. Cyclic voltammetry was carried out at room temperature (25°C) using saturated calomel electrode (SCE) as the reference electrode, a bright platinum foil as the counter electrode, and conducting glass as the working electrode. The Cd–Se–Te films were grown on the glass substrates under the conditions of controlled number of voltammetric scans (250–2,000) within the potential range of 0 to −1.0 V at a scan rate of 0.50 V/s using AUTOLAB 12 PG-stat, Eco-Chemie BV (The Netherlands). After deposition, the SC materials were rinsed with triple-distilled water and were air-dried.

Optical and microstructural characterizations

Reflectance spectra of the as-grown films were obtained with the help of a V-530 UV–VIS–NIR Spectrophotometer, JASCO (Japan), with a wavelength range of 350–1,100 nm. The band gap energy (E_g) was calculated from the plot of differential reflectance ($dR/d\lambda$) vs wavelength (λ). The SC films were subjected to scanning electron microscopy (SEM) analysis in a Hitachi S4500 FESEM to observe the morphology, and the composition was subsequently determined by energy dispersive analysis of x-ray (EDAX) using the same instrument. Philips PW 1710, an x-ray diffractometer using Cu Kα radiation of wavelength 1.5405 Å, was employed to study the crystallinity of the as-deposited thin films. The x-ray machine was operated at 25 kV and 20 mA within the 2θ range between 20° and 90° and 2θ increment of 0.02°. Atomic force microscopy (AFM) was performed on the prepared films using Dimension 3,000 Atomic Force Microscope (Digital Instruments, Santa Barbara, CA, USA) as detailed elsewhere [3, 4]. The thickness of the electrodeposited films was determined through focused ion beam (FIB) analysis with the help of FEI × P 200 focused ion beam miller using a fine (7 nm) beam of highly energetic (30 kV) gallium ions that scan over the surface of the specimen. The milling and imaging were performed at apertures of 2,700 and 14 pA, respectively [4, 5].
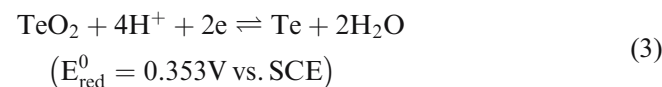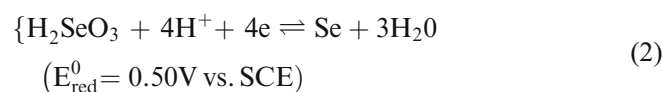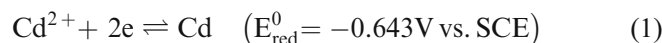
Electrochemical characterizations of the semiconductor electrode–electrolyte interface

The SC–electrolyte interface was characterized through electrochemical impedance spectroscopy (EIS) using AUTOLAB 12 PG-stat combined with a frequency response analyzer. A cell was fabricated with the configuration, (TCO) Cd–Se–Te | 0.5 M S^{2-}–S_x^{2-} | Pt, and the open circuit potential (OCP) was measured under illumination of 500 W m^{-2} for 30 min until a steady-sate potential is reached. The composition of the polysulfide solution in the cell was 0.5 M NaOH + 0.5 M Na_2S + 0.5 M S maintained at a pH of approximately 13.7. The impedance spectra at the respective OCPs were recorded applying sinusoidal perturbation of 5 mV amplitude in the electrolytic bath over a frequency range of 0.1 MHz to 20 mHz. The corresponding Nyquist plots were analyzed to evaluate the equivalent circuit (EC) parameters [4, 5, 20, 21]. Capacitance measurements of the SC electrode in contact with 0.5 M Na_2S_x electrolyte were performed using the same experimental setup with an oscillator frequency of 1 kHz, and the sinusoidal signal was kept constant at 20 mV peak-to-peak. The nature of the charge carriers and the donor densities of the SC materials were determined from the Mott–Schottky plots [5, 21]. The measurement of photoresponse in terms of rise and decay of short-circuit current (I_{sc}) was carried out with a similar cell setup using fresh SC surface under 500 W m^{-2} illumination. The decay constant (b) was evaluated from the plot of transient photoresponse, I_{sc}—time (t) at 20-s intervals in dark and illuminated conditions. Performance characteristic of the PEC cell was derived through $I–V$ measurement under similar illuminating condition.

Results and discussion

The typical cyclic voltammograms recorded for the electrodeposition of the Cd–Se–Te film on TCO-coated glass have been shown in Fig. 1, wherein a broad cathodic peak appears within the potential range of −0.50 to −0.85 V with respect to aqueous SCE. The reduction reactions associated with the film growth process are summarized below [22].

$$Cd^{2+} + 2e \rightleftharpoons Cd \quad \left(E_{red}^0 = -0.643 V \text{ vs. SCE} \right) \tag{1}$$

$$\{ H_2SeO_3 + 4H^+ + 4e \rightleftharpoons Se + 3H_2O \\ \left(E_{red}^0 = 0.50 V \text{ vs. SCE} \right) \tag{2}$$

$$TeO_2 + 4H^+ + 2e \rightleftharpoons Te + 2H_2O \\ \left(E_{red}^0 = 0.353 V \text{ vs. SCE} \right) \tag{3}$$

With further decrease of potential at around −1.0 V, a sharp decrease in current indicated H_2 evolution in the acid medium. The reverse anodic sweep resulted in Cd stripping, and the corresponding oxidation peak was observed at around −0.59 V.

The optical properties of the SC films grown under 250, 500, and 1,500 voltammetric cycles have been featured in the reflectance (%R) spectra (Fig. 2) by a broad absorption region in each case. This is indicative of codeposition of mixed/alloyed crystallites of CdSe, CdTe, and CdSeTe constituting the SC film matrix. The band gap energy (E_g)
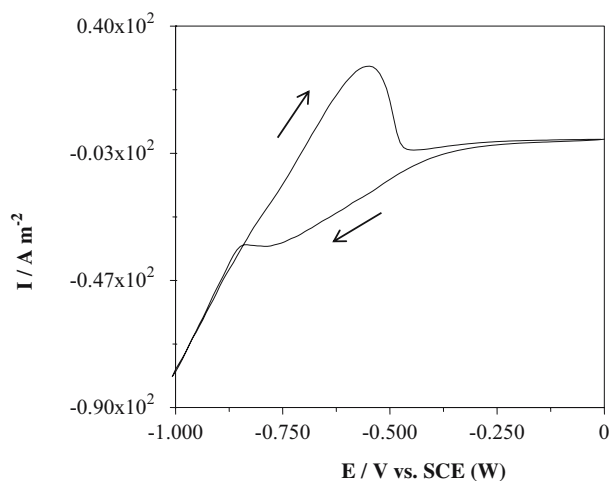
Fig. 1 Cyclic voltammograms for the electrodeposition of Cd–Se–Te on TCO-coated glass substrate

Table 1 Effect of the number of voltammetric cycles on the properties of SC thin film

Cycles	At.%			Band gap energy (eV)	Charge-transfer resistance (kΩ)		Efficiency (%)
	Cd	Se	Te				
250	39.7	0	60.3	1.0	1.5		0.40
500	50.0	13.8	36.2	0.6	1.4	1.7	0.42
1,000	38.0	30.0	32.0	1.9	1.4	1.7	0.37
1,500	39.4	10.5	50.1	2.6	1.4	1.7	0.38
2,000	55.7	12.2	32.1	3.1	1.5		0.26

values for the films are summarized in Table 1. It is observed that the film obtained at 250 periodic cycles is characterized by absorption corresponding to 1.4 eV only. For the rest of the films grown under an increased number of scans, the E_g values were obtained at approximately 1.4 as well as 1.7 eV. This observation further confirmed the formation of binary compounds CdTe and CdSe and the likely growth of the Cd–Se–Te alloyed system.

Typical SEM micrographs (Fig. 3a,b) of the films prepared under 500 and 1,500 cycles revealed a compact structure with densely packed microcrystals forming a homogeneous surface practically without cracks or holes. The micrograph in Fig. 3c represents an image in the inset at a much higher magnification (×30,000) of the sample prepared under 1,500 periodic cycles. The spherical nature of the particles with grain size in the order of 100 nm is discernable from the image. The elemental compositions of films were determined from the EDAX spectrum showing the existence of Cd–Se–Te with varying stoichiometry. Table 1 shows the variation of the atomic percent of Cd, Se, and Te, and Fig. 4 shows the variation of the atomic percent
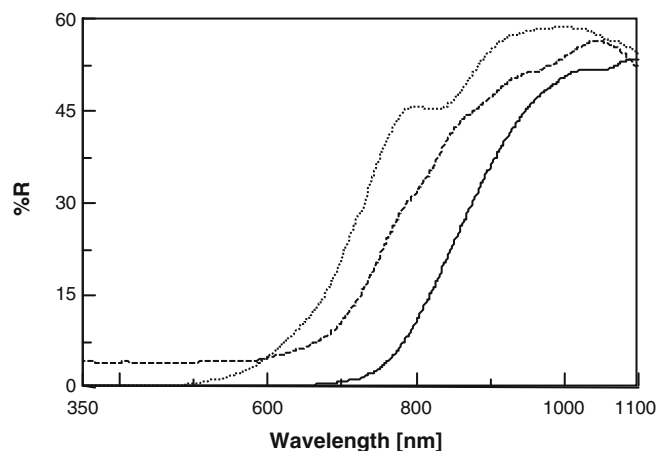
of Cd and (Se/Te) with the number of voltammetric cycles. It is interesting to note that the SC film developed through the minimum (250) periodic cycle does not contain Se in the matrix, which complies with the nonexistence of bandwidth for CdSe at 1.7 eV. When the number of scans was increased to 500, CdSe started growing within the matrix along with CdTe in larger quantity as has been evidenced from the EDAX data. Voltammetry under 1,000 periodic cycles yielded an SC matrix containing Cd, Se,
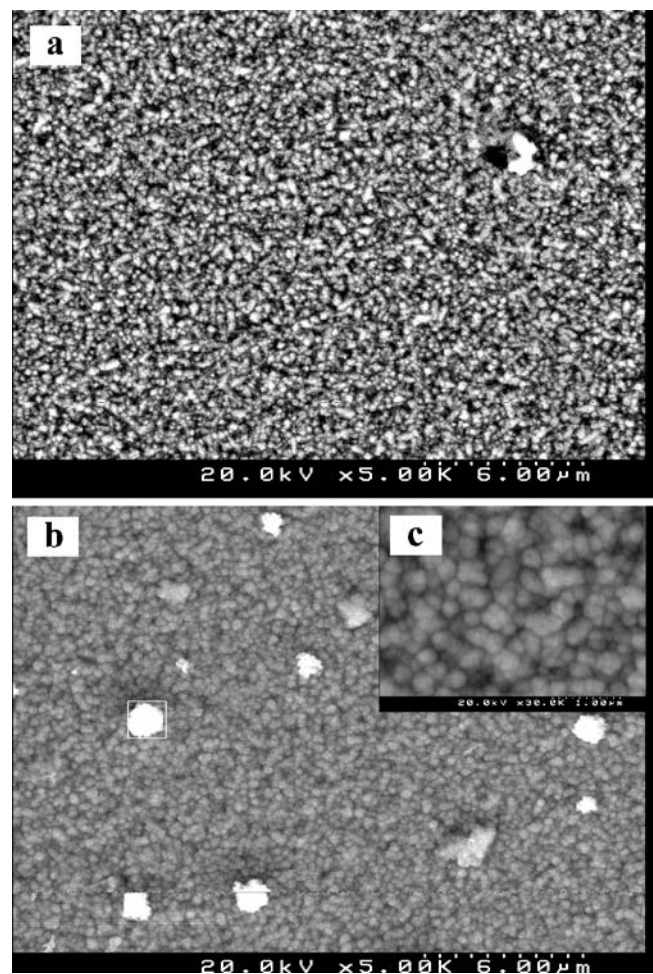

Fig. 3 Typical SEM images of the Cd–Se–Te film prepared under different periodic cycles. 500 (**a**), 1,500 (**b**), 1,500 (**c**, *inset*) cycles at higher magnification

Fig. 2 Reflectance spectra of Cd–Se–Te prepared at different voltammetric cycles (----- 250, —— 500, and — 1,500)
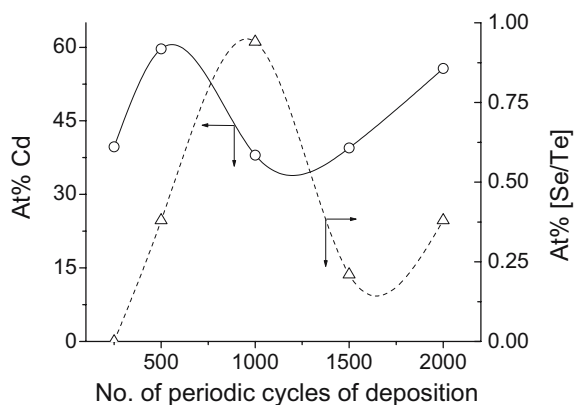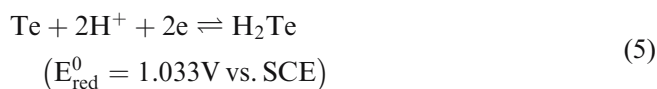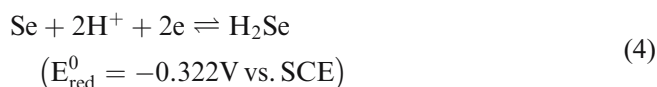
Fig. 4 Variation of the atomic percent of Cd and (Se/Te) with number of periodic cycles of deposition

and Te in almost equal stoichiometry, which is attributed to the formation of Se incorporated CdTe or a ternary alloy system Cd–Se–Te. However, for the materials prepared under 1,500 and 2,000 cycles of deposition, the removal of Se from the matrix occurred due to prolonged exposure in the aqueous acidic bath.

The positive reduction potential of the chalcogens along with their high electron affinity could be regarded as an effective phenomenon for the inclusion of more chalcogens rather than Cd in the film. However, the possible formation of hydrides of chalcogens in acid medium may also influence the film growth process by depletion of chalcogens from the matrix preferably in the order Se > Te as revealed from the following redox processes [22].

$$Se + 2H^+ + 2e \rightleftharpoons H_2Se$$
$$\left(E_{red}^0 = -0.322V \text{ vs. SCE}\right) \quad (4)$$

$$Te + 2H^+ + 2e \rightleftharpoons H_2Te$$
$$\left(E_{red}^0 = 1.033V \text{ vs. SCE}\right) \quad (5)$$

Thus, the variation of the atomic percent of (Se/Te) with number of voltammetric scans (Fig. 4) passes through a maximum at approximately 1,000 cycles that corroborates to the film composition $Cd_1Se_1Te_1$.

X-ray diffraction (XRD) analyses further confirm the nanostructure of the composite film composed of crystallites of ternary SCs Cd–Se–Te as well as the binary compounds CdSe and CdTe. Figure 5 represents the XRD plots for the materials prepared under different periodic cycles. A large number of XRD peaks, marked as 1,2,... in the figures, have been characterized with the help of Joint Committee for Powder Diffraction Standards (JCPDS) data file and have been summarized in Table 2 [23–30]. Mixed or alloyed ternary phases, namely, $CdSe_{0.6}Te_{0.4}$, $CdSe_{0.1}Te_{0.9}$, etc., along with various CdSe and CdTe were identified through the lattice parameters. However, some of the peaks in the plot could not be characterized due to dearth of sufficient literature data on mixed or alloyed ternary
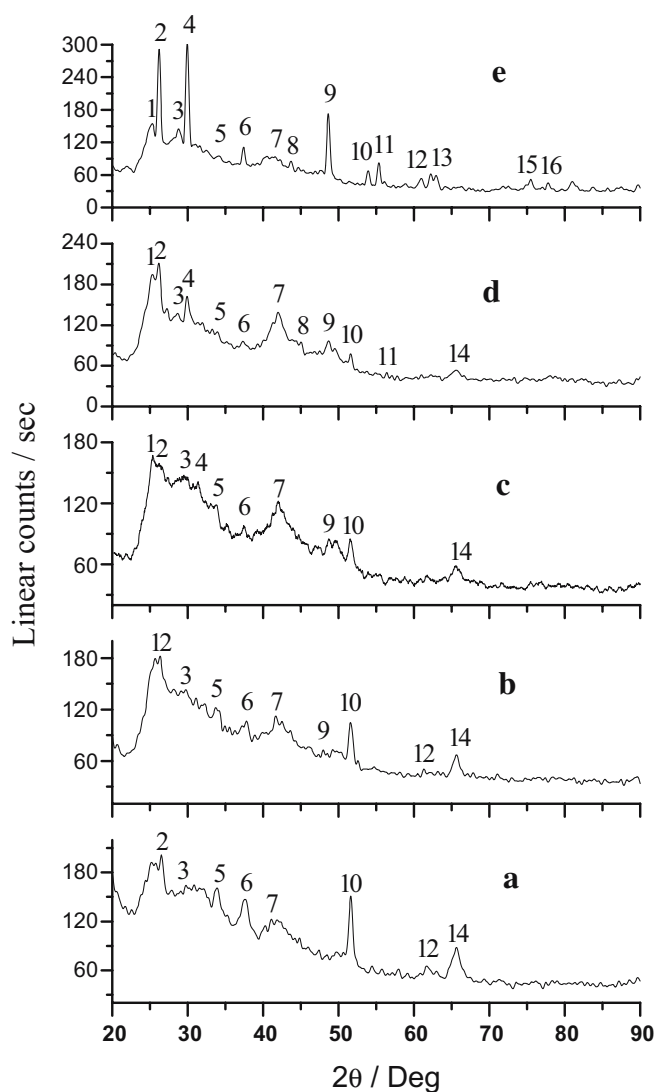

Fig. 5 XRD pattern of the materials prepared under different periodic cycles. 250 (**a**), 500 (**b**), 1,000 (**c**), 1,500 (**d**), and 2,000 (**e**) cycles of deposition

compounds, and discussions on these peaks could not be included in this section.

It may be noted that neither $CdSe^h$ nor $CdSe^c$ (identified as peak 1) appears in the XRD regime obtained with lower periodic scans (250 cycles). This complies with the EDAX results that selenide compounds do not exist in sufficient amount in such film matrix. During successive prolonged periodic scans, peaks 2 and 9 get intensified, supporting the formation of ternary phases along with binary compounds. The predominance of ternary phases with greater number of cycles is further evidenced by the decline of peak 10. It may be understood that besides the formation of ternary crystals, there is possible alloying of the binary crystallites to the ternary phases.

Figure 6a,b shows the topographic AFM images of the as-grown films synthesized under 250 and 1,000 cycles. The films are found to be composed of small spherical particles of approximately 80-nm average grain size. Uni-

Table 2 Results of XRD analyses of the SC films prepared under different periodic cycles

Peak number	250	500	1,000	1,500	2,000	Identification of the crystallites
1	–	3.52	3.51	3.52	3.52	$CdSe^h$ (002), $CdTe^h$ (101), $CdSe^c$ (111), $CdSe_{0.6}Te_{0.4}$ (002)
2	3.36	3.39	3.39	3.40	3.40	$CdSe_{0.6}Te_{0.4}$ (101)
3	3.07	3.07	3.08	3.11	3.10	Undefined
4	–	–	3.02	2.98	2.98	Se^h (101)
5	2.64	2.66	2.65	2.64	2.63	$CdTe^t$ (101), $CdSe_{0.6}Te_{0.4}$ (102)
6	2.39	2.38	2.40	2.41	2.40	Te^h (102)
7	2.20	2.17	2.15	2.15	2.17	$CdSe_{0.6}Te_{0.4}$ (110), Se^h (110)
8	–	–	–	–	2.07	$CdSe_{0.6}Te_{0.4}$ (111), Se^h (102)
9	–	1.90	1.87	1.87	1.87	$CdSe^h$ (200), $CdSe_{0.6}Te_{0.4}$ (112)
10	1.77	1.77	1.77	1.77	1.78	$CdTe^h$ (202), Te^h (112), Se^h (201)
11	–	–	–	1.63	1.66	$CdSe^h$ (202), Se^h (003)
12	1.52	1.52	–	–	1.52	$CdTe^h$ (203), $CdSe^c$ (400)
13	–	–	–	–	1.49	$CdTe^h$ (210), $CdTe^c$ (331), $CdSe_{0.1}Te_{0.9}$ (203)
14	1.42	1.42	1.42	1.42	–	$CdSe^h$ (203), $CdTe^h$ (105), $CdSe^c$ (331), $CdSe_{0.6}Te_{0.4}$ (210)
15	1.29	–	–	–	1.26	$CdSe^h$ (300), $CdTe^h$ (006), $CdTe^c$ (511), $CdSe_{0.6}Te_{0.4}$ (002)
16	–	–	–	–	1.19	$CdSe^h$ (302), $CdTe^h$ (220)
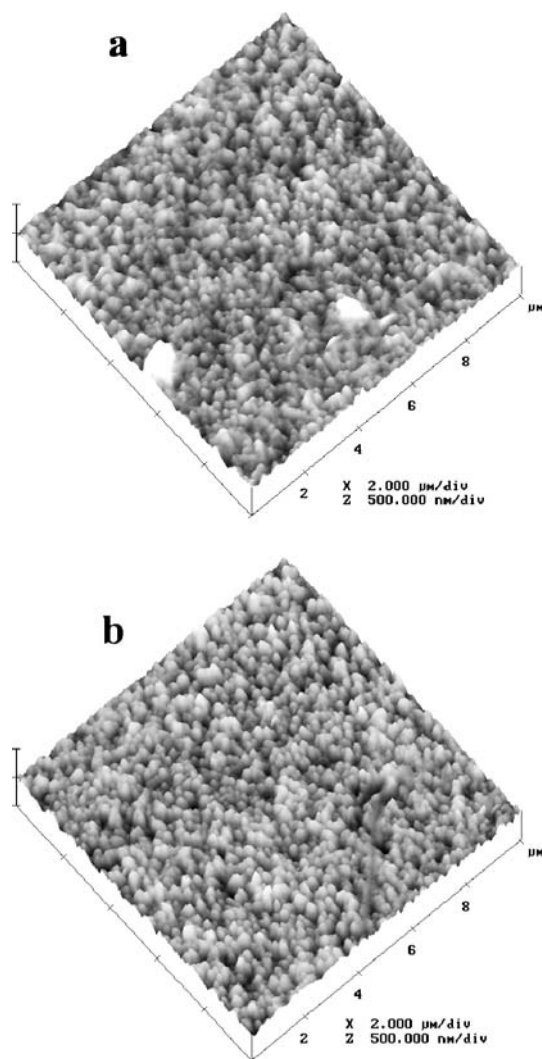
Fig. 6 a, **b** Typical AFM images of the Cd–Se–Te film prepared under 250 and 1,000 voltammetric cycles

formity in film thickness is visible from the typical FIB images shown in Fig. 7a,b. It is interesting to note that the thickness increased fairly linearly with increased number of voltammetric scans in the order of 22 nm/100 cycles of deposition as shown in Fig. 8. Such a plot may be considered to be a calibration curve to obtain an SC film with desired thickness and stoichiometry.

Notably the films produced from different periodic cycles were found to differ in character as regard to semiconducting properties (e.g., carrier density, carrier lifetime) and PEC output characteristics (e.g., charge-transfer resistance, photoconversion efficiencies). Measurement of capacitance vs applied potential gave useful information regarding types of conductivity of the deposits and the carrier concentrations, which were derived from the slope of the Mott–Schottky plots using the relation [3, 5, 21]

$$C_{SC}^{-2} = (V - V_{fb} - k_B Te^{-1}) 2(\varepsilon_0 \varepsilon_S N_D e)^{-1} \qquad (6)$$

where V and V_{fb} denote the electrode potential and the flat-band potential, respectively; ε_0 and ε_s are the permittivities in vacuum and in the SC electrode respectively; e is the carrier charges; T is the operating temperature (298 K); k_B is the Boltzmann's constant; and C_{SC} is the space charge capacitance. Figure 9 resembles a typical Mott–Schottky plot for the synthesized films at 250, 500, and 1,500 periodic cycles. The positive slope of the plot confirms n-type conductivity of the deposits. The nonlinearity in the plots is ascribed due to various factors like surface roughness, uneven doping, and specific adsorption of the redox species at the surface of the as-grown SC films used in the PEC cell. In the course of the present investigations on capacitance measurement of the films deposited on the SnO_2-coated glass substrate, there was hardly any significant contribution made by the bare TCO-coated surface to the Mott–Schottky capacitance. Hence, the effect of TCO was ignored in such experiment. The variation of donor
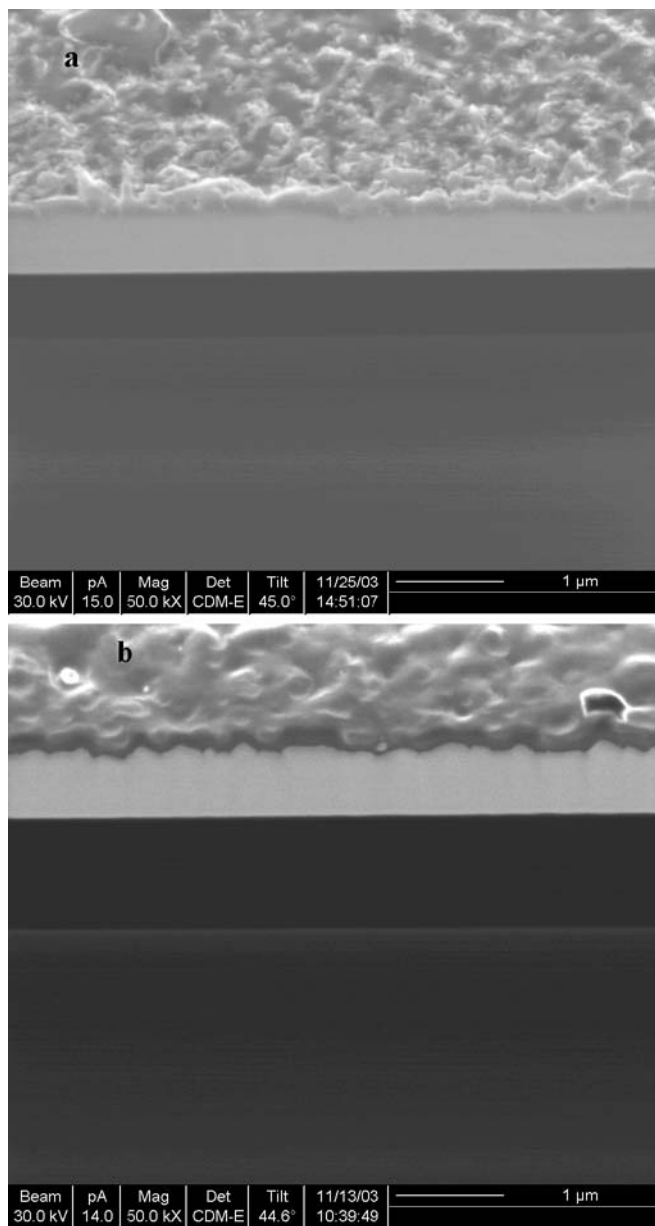
Fig. 7 a, b Typical FIB images of the Cd–Se–Te film prepared under 500 and 2,000 voltammetric cycles
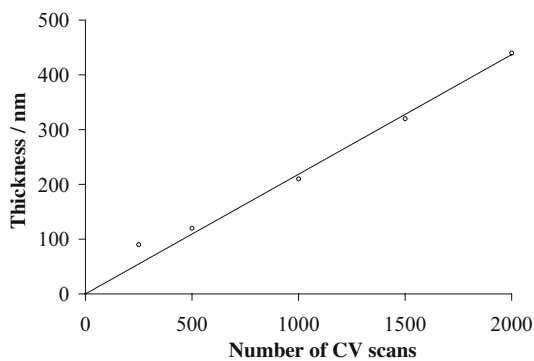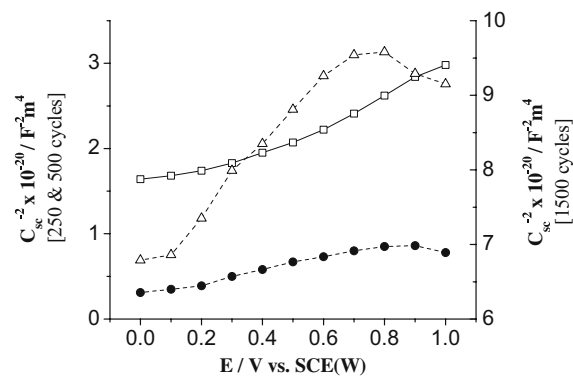

Fig. 9 Mott–Schottky plot for the TCO|Cd–Se–Te|0.5 M S^{2-}–S_x^{2-}|Pt system (–□– 250, --•-- 500, and --Δ-- 1,500 periodic cycles of deposition)

concentration (N_D) with number of depositing cycles has been presented in Fig. 10. It is observed that N_D passes through a maximum at approximately 500 cycles of deposition.

Stable short-circuit current (I_{sc}) was recorded for the PEC cell, (TCO) Cd–Se–Te|0.5 M S^{2-}–S_x^{2-}|Pt, during alternate exposure of darkness and illumination of the anode chamber. Figure 11 depicts the typical rise and decay characteristics of I_{sc} values for the PEC cell fabricated with the films prepared under 500 and 1,000 periodic cycles. Dependence of I_{sc} with t was found to follow the relation

$$I_{sc}(t) = I_{sc}(0)t^{-b} \tag{7}$$

where $I_{sc}(t)$ and $I_{sc}(0)$ are the short-circuit current at time t and zero seconds, respectively, and b is the decay constant [31]. The b values for different films were obtained from the linear plots of $\log(I_{sc})$ vs log t plot (Fig. 12). Voltammetric scans within the range of 500–1,000 periodic cycles were found to impart significant photosensitivity to the films as observed by the maximum in the b values shown in Fig. 10.

The influence of the number of cycles on the feasibility of charge transfer across the SC–solution interface was
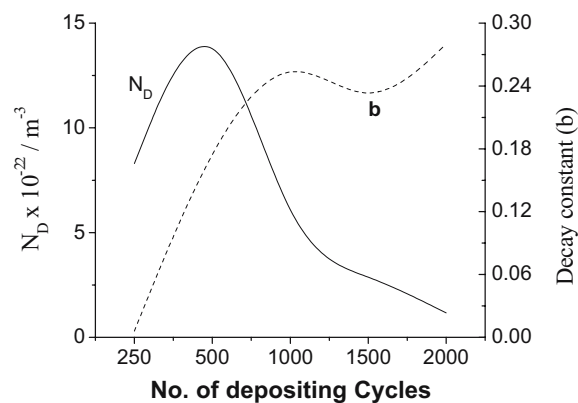

Fig. 8 Variation of film thickness with number of cycles of deposition

Fig. 10 Variation of donor density and decay constant with number of cycles of deposition
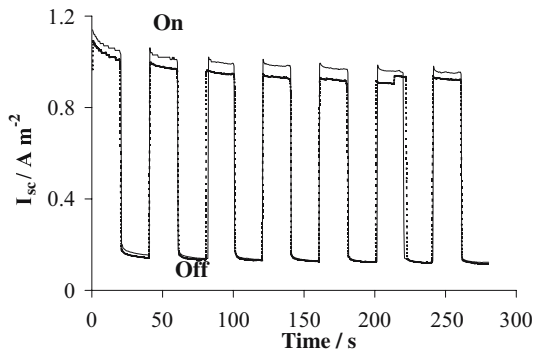
Fig. 11 Short-circuit current (I_{sc})—rise and decay curves for n-Cd–Se–Te/polysulphide PEC cells (•••• 500 and – – 1,000 periodic cycles of deposition)

Fig. 13 **a** Typical Nyquist plot for the n-Cd–Se–Te/0.5 M S^{2-}–S_x^{2-} system (Δ Δ 500, ∘ ∘ 1,000, and + + 2,000 cycles of deposition). **b** EC diagram (*inset*)

revealed through EIS measurements. Typical Nyquist plots shown in Fig. 13a exhibited more or less a similar structure across the SC–0.5 M Na_2S_x solutions interface for different films [4, 5, 20]. The impedance data were further analyzed based upon the simple EC model (Fig. 13b). The circuit includes a solution resistance (R_s), charge-transfer impedance (R_{ct}), and a double layer capacitance associated with the charge-transfer process (C_{ct}) [4, 5, 20, 21, 32]. In fact, a material with low values of R_{ct} is generally considered suitable as PEC cell component for the pronounced ability in conducting charges. R_{ct} values for the prepared films have been displayed in Table 1. The films prepared under 500–1,000 cycles showed considerably low R_{ct} values (approximately 0.6 kΩ) in contrast with those obtained from 1,500 and 2,000 cycles, which showed R_{ct} values as high as 2.6 and 3.1 kΩ, respectively, and corresponded to poor performance in the PEC cell.

To derive the photoconversion efficiency (%η), the fabricated PEC cells were subjected to current–voltage measurements (Fig. 14) under illumination of 500 W m^{-2}, and %η values are shown in Table 1. The films obtained under periodic cycles of approximately 500 exhibited a maximum efficiency of 0.42%. This may be attributed to the synergic effect of the properties like (i) maximum donor density (17.6×10^{22} m^{-3}) [19], (ii) minimum charge-transfer

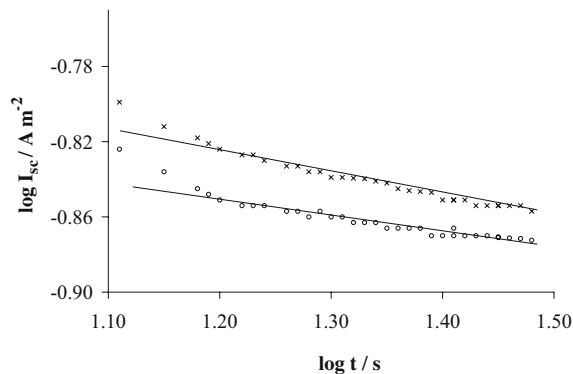resistance (0.6 kΩ), and (iii) sufficiently high lifetime of the carriers or low decay constant value (0.19), which characterizes the film for potential PEC applications.

Conclusions

Voltammetry over controlled periodic cycles can provide a simple and cost-effective method for developing SC thin films on conducting glass substrates. Over a period of 500 cycles, the formation of mixed compounds of CdSe and CdTe is highly probable as suggested from the EDAX analysis, whereas growth of Cd–Se–Te ternary compounds are evident under 1,000 periodic cycles. The deposition process is associated with several competing phenomena under a span of potential. Thus, it may favor the formation of binary or ternary compounds depending upon the duration or number of cycles of deposition. These binary and ternary chalcogenide compounds are found to grow into the film matrix in the form of micro-/nanocrystallites with an average particle size of approximately 80 nm. The composite film exhibits a wide range of absorption spectra from 1.4 to 1.7 eV. The blended structure of the film matrix
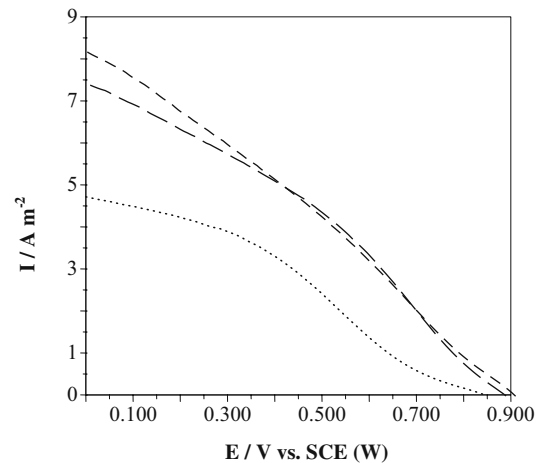

Fig. 12 Variation of log (I_{sc}) vs log t (–×– 500 and –∘– 1,000 periodic cycles of deposition)

Fig. 14 Typical I–V curves for the n-Cd–Se–Te/polysulphide PEC cells (— — 250, – – 500, and ······· 2,000 cycles of deposition)

shows promising PEC performances with n-type conductivity when investigated at electrode–electrolyte interfaces. Thus, it may be concluded that the optimum range of 500–1,000 periodic cycles effectively controls the composition and structure of the films and imparts desirable properties for their PEC applications.

References

1. Bard AJ, Wrighton MS (1977) J Electrochem Soc 124:1706
2. Bouroushian M, Charoud-Got J, Loizos Z, Spyrellis N, Maurin G (2001) Thin Solid Films 381:39 (and relevant references therein)
3. Bhattacharya C, Datta J (2005) Mater Chem Phys 89:170 (and relevant references therein)
4. Datta J, Bhattacharya C, Bandyopadhyay S (2004) In: Proceedings of the international conference on nanomaterials: synthesis, characterization and application, 4–6 Nov, Kolkata, Tata. McGraw-Hill, New Delhi, pp 426–431
5. Datta J, Bhattacharya C, Bandyopadhyay S (2005) Appl Surf Sci (in press). DOI 10.1016/j.apsusc.2005.09.006 (available online; and relevant references therein)
6. Benamar E, Rami M, Fahoume M, Chraibi F, Ennaoui A (2000) M J Condens Mater 3:71
7. Das VD, Damodara L (1998) Mater Chem Phys 56:116 (and relevant references therein)
8. Patil VB, Shahane GS, Deshmukh LP (2003) Mater Chem Phys 80:625 (and relevant references therein)
9. Murali KR, Subramanian V, Srinivasan K (1999) J Mater Sci 34:3417
10. Shen CM, Zhang XG, Li HL (2005) Appl Surf Sci 240:34
11. Roy UN, Babalola OS, Cui Y, Groza M, Mounts T, Zavalin A, Morgan S, Burger A (2004) J Cryst Growth 265:453
12. Premaratne K, Akuranthilaka SN, Dharmadasa IM, Samantilleka AP (2004) Renew Energy 29:549
13. Velumani S, Mathew X, Sebastian PJ (2003) Sol Energy Mater Sol Cells 76:359
14. Matsumura N, Sakamoto T, Saraie J (2003) J Cryst Growth 251:602
15. Pena DJ, Mbindyo JKN, Carado AJ, Mallouk TE, Keating CD, Razavi B, Mayer TS (2002) J Phys Chem 106:7458
16. Kressain AM, Doan VV, Klein JD, Sailor MJ (1991) Chem Mater 3:1015
17. Bouroushian M, Kosanovic T (2005) J Solid State Electrochem (in press). DOI 10.1007/s10008-005-0670-x
18. Bouroushian M, Kosanovic T, Spyrellis N (2005) J Solid State Electrochem 9:55
19. Cachet H, Cortes R, Froment M, Maurin G (1997) J Solid State Electrochem 1:100
20. Datta J, Bhattacharya C, Bandyopadhyay S (2005) Bull Mater Sci 28:253
21. Memming R (2000) Semiconductor Electrochemistry. Wiley, Canada
22. Lide DR (1998) Handbook of chemistry and physics, 79th edn. CRC, Boca Raton, pp 8.22–8.25
23. JCPDS file for CdSe: 08-0459
24. JCPDS file for CdSe: 19-0191
25. JCPDS file for CdTe: 19-0193
26. JCPDS file for CdTe: 15-0770
27. JCPDS file for Se: 42-1425
28. JCPDS file for Te: 08-0459
29. JCPDS file for $CdSe_{0.6}Te_{0.4}$: 41-1325
30. JCPDS file for $CdSe_{0.1}Te_{0.9}$: 41-1324
31. Jadhav US, Kale SS, Lokhande CD (2001) Mater Chem Phys 69:125
32. Cruz J, Garcia-choa E, Castro M (2003) J Electrochem Soc 150:B26